CsoR Is Essential for Maintaining Copper Homeostasis in *Mycobacterium tuberculosis*

Sarah A. Marcus, Sarah W. Sidiropoulos¤, Howard Steinberg, Adel M. Talaat*

Department of Pathobiological Sciences, University of Wisconsin-Madison, Madison, Wisconsin, United States of America

¤ Current address: Oakland Community College, Auburn Hills, Michigan, United States of America
* atalaat@wisc.edu

Abstract

Mycobacterium tuberculosis, a pathogen infecting one third of the world population, faces numerous challenges within the host, including high levels of copper. We have previously shown that *M. tuberculosis* CsoR is a copper inducible transcriptional regulator. Here we examined the hypothesis that *csoR* is necessary for maintaining copper homeostasis and surviving under various stress conditions. With an unmarked *csoR* knockout strain, we were able to characterize the role of *csoR* in *M. tuberculosis* as it faced copper and host stress. Growth under high levels of copper demonstrated that *M. tuberculosis* survives copper stress significantly better in the absence of *csoR*. Yet under minimal levels of copper, differential expression analysis revealed that the loss of *csoR* results in a cell wide hypoxia-type stress response with the induction of the DosR regulon. Despite the stress placed on *M. tuberculosis* by the loss of *csoR*, survival of the knockout strain was increased compared to wild type during the early chronic stages of mouse infection, suggesting that *csoR* could play an active role in modulating *M. tuberculosis* fitness within the host. Overall, analysis of CsoR provided an increased understanding of the *M. tuberculosis* copper response with implications for other intracellular pathogens harboring CsoR.

Introduction

Mycobacterium tuberculosis is one of the world's most successful bacterial pathogens, infecting approximately one third of the human population. Despite widespread vaccination and the existence of antibiotic therapies, this causative agent of tuberculosis leads to over 1 million deaths each year [1]. Part of the success of this pathogen is attributed to its ability to quickly adapt and survive within harsh host microenvironments. The stress conditions *M. tuberculosis* must face within the host include reactive nitrogen and oxygen species [2], low pH [3], and hypoxia [4]. Recently, copper has been recognized as an additional weapon in the host macrophage's arsenal as it localizes high levels of copper to the mycobacterial phagosome [5]. This finding led our group to investigate the *M. tuberculosis* response to copper stress revealing a set of 30 genes responsive to copper and the damage it can cause [6]. Among these genes were two that encode for copper-responsive transcriptional repressors—paralogs now identified as *ricR* and *csoR*—the latter of which we continue to characterize in this report.

The bactericidal capabilities of copper have been known for some time [7]. The mechanisms of copper damage include production of oxidative stress through Fenton reactions [8], displacing metal cofactors in proteins, and destabilization of Fe-S clusters [9]. Indeed, high physiological levels of copper have been demonstrated to be bactericidal for *M. tuberculosis* [5, 6]. Conversely, copper serves as a cofactor of metalloenzymes and is necessary in trace amounts for various cellular activities [10]. In *M. tuberculosis* such metalloenzymes include cytochrome *c* oxidase and superoxide dismutase [11], thus the role of copper in metabolism and the copper stress response must be carefully regulated. For example, under hypoxic conditions, which increase copper toxicity, *M. tuberculosis* makes use of copper-independent cytochrome *bd* oxidase [12]. This effectively reduces the requirement for cytochrome *c* oxidase, and therefore copper, under conditions where copper poses the greatest threat to the cell.

To better understand how the copper stress response is managed, we began to characterize one *M. tuberculosis* copper-induced regulator, CsoR. The crystal structure of CsoR revealed that the protein forms a homodimer with each monomer binding one molar equivalent of Cu (I) [13]. In its apo form, CsoR binds the promoter of its own copper-sensitive operon (*cso*), however upon binding copper, repression is released inducing expression of the *cso* in a graduated manner leading to the export of copper ions. Here we investigated the importance of the negative regulatory role of *csoR* in *M. tuberculosis* copper homeostasis. Our initial results, examining the Δ*csoR* strain under copper stress and during early chronic murine infection, suggested that under certain conditions *M. tuberculosis* may have an advantage upon suppressing the expression of *csoR*. Closer examination of the transcriptome of *M. tuberculosis* lacking *csoR*, however, revealed a hypoxic stress response during growth in copper-free media. This response may have better prepared the bacilli for survival during the early chronic stage of murine infection. We expect that *M. tuberculosis* must strike a balance when it comes to handling copper stress and that CsoR is integral, though perhaps not alone, in this role. Furthermore, in this role CsoR may make an important contribution during entry to the chronic phase of tuberculosis.

Results

Generation of *M. tuberculosis csoR* constructs

To create a knockout mutant of *csoR* in the virulent, wild type *M. tuberculosis* strain H37Rv, homologous recombination was used to replace 5 base pairs (bp) of the 360bp coding region of *csoR* with a hygromycin resistance cassette (*hyg_R*), an ~2.4kB region, using the cosmid pYUB854 (Fig 1A) [14]. The mutant was confirmed by sequencing and with Southern blot, which showed a 2.4kB shift between bands from wild type or mutant strains (Fig 1B). However, reverse transcriptase PCR (RT-PCR) testing for expression of the downstream genes revealed loss of transcription of all three downstream genes in the *cso*: Rv0968, a conserved hypothetical protein; *ctpV*, coding for a copper-exporter [15]; and Rv0970, a conserved membrane protein of unknown function (Fig 1C). In order to create a nonpolar Δ*csoR* strain, an additional step was taken to remove the hygromycin cassette. The vector pYUB870 [14] was electroporated into Δ*csoR*::*hyg_R* removing *hyg_R* and leaving behind a 150 bp insertion sequence at the 14th codon of *csoR*. The resulting unmarked mutation led to a frame shift which introduced 6 stop codons either at the insertion site or within the remainder of the *csoR* gene. RT-PCR results confirmed transcription of the remaining members of the *cso* in the unmarked mutant strain (Fig 1C). A complementation strain, Δ*csoR*::*csoR*, was constructed by incorporating *csoR* under its own promoter into the Δ*csoR* genome using the integrative vector pMV306.

To ensure that no other possible disruptions of the genome in or outside of the *cso* were contributing to the examined phenotypes, whole genome sequencing was carried out
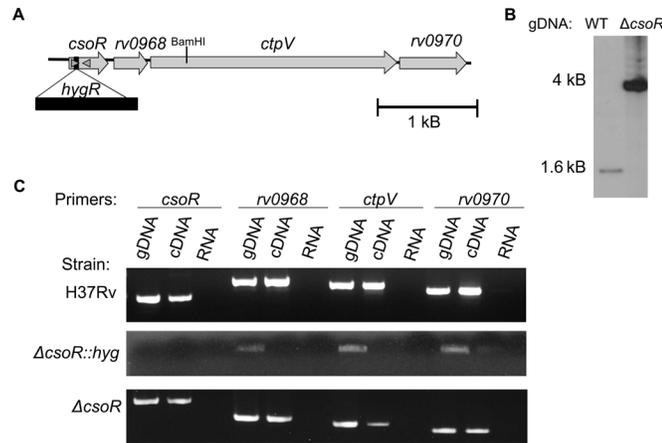
Fig 1. Construction of a nonpolar *M. tuberculosis* ΔcsoR strain. (A) Diagram showing the copper-sensitive operon drawn to scale. To knock out *csoR*, the first gene of 4 in its operon, a 2.4kB hyg_R cassette (black bar) was inserted near the 5' region of *csoR*. Grey arrowheads indicate primers flanking the genomic region amplified to be used as a probe for Southern blot. The BamHI cut site within the *cso* used for Southern blot is shown. **(B)** Southern blot targeting the *csoR* region after BamHI digestion of wild type (WT) or ΔcsoR::hyg_R genomic DNA (gDNA) demonstrating insertion of the hyg_R cassette. **(C)** The polar nature of the different ΔcsoR constructs was tested by RT-PCR of H37Rv, ΔcsoR::hyg_R, and ΔcsoR after exposure to 500µM $CuCl_2$, with gDNA positive and RNA negative controls from the same strains.

doi:10.1371/journal.pone.0151816.g001

comparing *M. tuberculosis* ΔcsoR with its wild type H37Rv parent strain. A total of 95 single nucleotide polymorphisms (SNPs) were found in *M. tuberculosis* ΔcsoR when compared to the published H37Rv reference [16]. Of these, 38 SNPs corresponded to those identified as sequencing errors in the original reference [17] and 49 of the remaining SNPs were found in the sequenced parent strain. In all 8 unique SNPs were found in *M. tuberculosis* ΔcsoR differentiating it from the parent strain. Two of these SNPs had been previously identified as they were annotated at the start of the insertion sequence in *csoR*. Five of the other six SNPs were found to be non-synonymous. One SNP each was found in PPE5 (Rv0304c) and PPE55 (Rv3347c). Three more, including the one synonymous SNP, were found in PE_PGRS9 (Rv0746). The last was found in a probable cyclase, Rv2435c. When *M. tuberculosis* ΔcsoR was searched for larger genomic variations, only the 150bp scar at the *csoR* deletion site was identified. Given the distance of these variations from the *cso* and the function of the genes they target, it seems unlikely that the observed phenotypes could be due to anything other than the deletion of *csoR*.

Survival of ΔcsoR is enhanced under copper stress

To test the growth kinetics of *M. tuberculosis* ΔcsoR during copper stress, wild type and mutant strains were grown in copper-free Sauton's liquid media with no added copper or with 50 or 500µM $CuCl_2$. As expected, both strains showed similar levels of growth in untreated cultures suggesting no generalized growth defects (Fig 2A), and showed a decline in growth in the presence of 500µM $CuCl_2$ (Fig 2B). While the gradual decline of the ΔcsoR strain in 500µM $CuCl_2$ was similar to wild type at early time points, by day 15 the culture of the knockout strain maintained its total CFU/ml while the wild type culture continued to decline (Fig 2B). The difference at this time point was significant ($P = 0.002$) and observed across two separate experiments. Growth of the two strains in 50µM $CuCl_2$ did not vary from that of untreated cultures (S1 Fig).

To investigate the possibility that *csoR* and its regulon may play a greater role during later stages of growth as the culture transfers into stationary phase, the growth curves were repeated
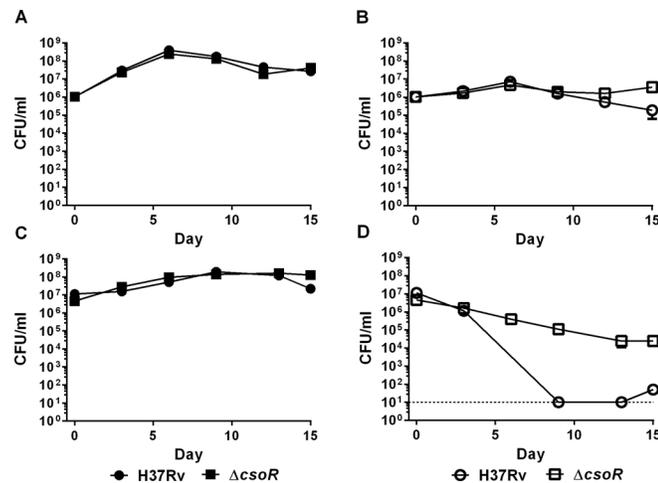
Fig 2. Growth kinetics of ΔcsoR under copper stress. (A) Growth of *M. tuberculosis* H37Rv (circles) and
Δ*csoR* (squares) over the course of 15 days in Sauton's media left untreated (filled), or **(B)** treated with
500μM CuCl$_2$ (open). **(C)** Growth of stationary phase *M. tuberculosis* H37Rv (circles) and Δ*csoR* (squares)
inocula over the course of 15 days in Sauton's media left untreated (filled), or **(D)** treated with 500μM CuCl$_2$
(open). The dashed line indicates the limit of detection. Shown are one of two similar biological replicates with
error bars representing standard deviation.

doi:10.1371/journal.pone.0151816.g002

inoculating from cultures that had reached stationary phase, rather than from actively growing
cultures as was done above. Interestingly, the difference in survival between *M. tuberculosis*
wild type and Δ*csoR*, while not affected in untreated cultures (Fig 2C), differed dramatically in
the presence of 500μM CuCl$_2$ (Fig 2D). This difference was noted after day 4 when wild type
survival fell two logs lower than the mutant. By day 8 it remained near the limit of detection, 10
CFU/ml, while Δ*csoR* survival declined much more gradually, remaining above 10^4 CFU/ml
through day 15, indicating the ability of Δ*csoR* to adapt to increased Cu levels.

After testing survival under two concentrations of copper, we sought to investigate the
impact of copper on the growth of *M. tuberculosis* Δ*csoR* at a higher resolution. This was done
by employing a modified microplate Alamar blue assay (MABA) [18, 19]. Growth inhibition of
M. tuberculosis wild type H37Rv, Δ*csoR*, and Δ*csoR::csoR* by two-fold dilutions of CuCl$_2$ rang-
ing from 16μM to 4000μM was tested (S2 Fig). Microplates were inoculated with cultures
growing at mid-log phase and read after approximately 10 days of growth. Susceptibility of
both wild type and complement strains was equivalent, both showing a minimum inhibitory
concentration (MIC) of 250μM CuCl$_2$. The mutant, on the other hand, showed an MIC of
500μM CuCl$_2$. These data confirmed the idea that loss of *csoR* improves survival of *M. tubercu-
losis* under copper stress.

Absence of *csoR* improves survival of *M. tuberculosis* during the early stages of chronic infection

To gain a broader understanding of the role of *csoR* during *M. tuberculosis* infection, BALB/c
mice were infected with H37Rv wild type or Δ*csoR* by aerosol infection. The groups infected
with wild type received on average 370 CFU per animal while Δ*csoR* infected mice received
closer to 1500 CFU per animal; however this difference in inoculum did not reach significance.
In fact, by week 2 Δ*csoR* showed on average slightly less colonization than wild type. Despite
this early trend, by weeks 4 and 8 Δ*csoR* showed a significant increase in survival compared to
wild type (*P* = 0.015 and *P* = 0.005 respectively). This increase, however, was not sustained
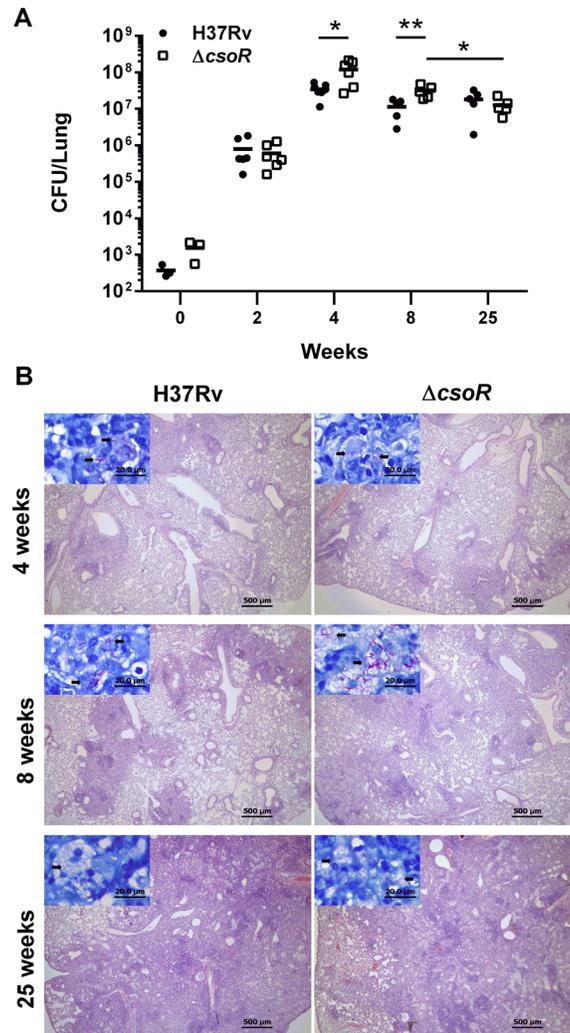
Fig 3. Growth of Δ*csoR* in the lungs during mouse infection. (A) Groups of BALB/c mice were infected by aerosol route with either *M. tuberculosis* H37Rv (filled circles) or Δ*csoR* (open squares). Shown are CFU per lung for each individual mouse over the course of 25 weeks across two independent experiments. Asterisks indicate significance with the following *P*-values: * $P < 0.015$; ** $P < 0.005$. **(B)** Histopathology for mice infected with H37Rv or Δ*csoR* at 4 and 8 weeks. Mouse lung sections were stained with H&E and are shown at 40× magnification (scale bar = 500μm). Insets show Ziehl-Neelson stained sections of lung tissue with pink bacilli indicated by black arrows at 1000× magnification (scale bar = 20μm).

long term, as by week 25 no significant difference in survival between wild type and knockout was apparent ([Fig 3A](#)). While the colonization of the wild type strain was consistent from week 8 to week 25, Δ*csoR* showed a significant drop from week 8 to week 25 ($P = 0.007$), suggesting that the improved growth rate during early chronic stage was not sustainable throughout the duration of chronic infection. Unlike the lungs, no significant difference in survival was seen between wild type and Δ*csoR* when spleen and liver were assayed, although mean CFU/g were consistently higher in the mutant strain in both organs ([S3 Fig](#)). Body weight of the mice did not vary significantly between groups after week 2 of the experiment, when mice infected with ΔcsoR were on average 1.2g lighter than those infected with wild type ($P = 0.005$) ([S3 Fig](#)). His-topathology of the lungs, spleen, and liver ([Fig 3B](#)) was scored by a trained pathologist. For both strains, lymphocytic infiltration and granulomatous reaction in the lungs worsened as the

infection progressed, while minimal pathology was seen in the spleen and liver. No significant difference was noted between strains at any time point for any of the tissues (S4 Fig). In sum, *csoR* conferred a moderate disadvantage to wild type *M. tuberculosis* during the early weeks of murine infection, but may be required for long term survival.

The global transcriptional response of *M. tuberculosis* Δ*csoR*

To better understand the breadth of influence *csoR* has directly as a regulator, and indirectly over copper homeostasis within the cell, the Δ*csoR* transcriptome was interrogated and compared to that of wild type *M. tuberculosis* H37Rv using RNA-Seq analysis. Our previous work [13] and that concerning *csoR* in other species such as *B. subtilis* [20] has suggested that under copper stress CsoR derepresses its regulon, and therefore few transcriptional differences between wild type and *csoR* knockout strains would be noted when compared under copper stress. Thus, we compared the transcriptomes of both wild type *M. tuberculosis* and Δ*csoR* grown in copper-free Sauton's media. Details of the number of reads and how they mapped can be found in S1 Table. Differential expression analysis using strict cutoffs requiring differentially expressed genes to have a fold change $\geq |2.0|$ and a false discovery rate (FDR) of ≤ 0.05 left us with 223 genes that were significantly, differentially expressed between the mutant and wild type strains (S2 Table). Of those genes 152 were induced, while 71 were repressed in Δ*csoR* compared to wild type (Fig 4A). To confirm these results, 10 genes were selected– 6 induced and 4 repressed–for quantitative, real-time PCR (qRT-PCR). All 10 were confirmed to be induced or repressed in the same direction, and with similar magnitude as the RNA-Seq data (S5 Fig).

It has already been established by our group and others that *csoR* represses its own operon in the absence of copper [13, 21]. Therefore, we first looked at the expression levels of the *cso*. As expected under low levels of copper, the *cso* was moderately induced in the Δ*csoR* strain as compared to wild type (Fig 4A; Table 1). This included the observed induction of *csoR* itself as sufficient remnants of the mutated *csoR* gene remained for successful RNA-Seq analysis. As CsoR is an established copper-responsive regulator, the list of differentially expressed genes in Δ*csoR* compared to wild type was interrogated for the 30 genes known to be responsive to copper in *M. tuberculosis* as determined by previous microarray analysis [6]. Very few genes overlapped; in fact, the only overlapping gene outside of the *cso*, Rv0848, was repressed in the Δ*csoR* strain despite being induced under copper stress (Fig 4A and 4B; Table 1). These results suggest that *csoR* may indeed only directly control expression of its own operon as previously suggested by Festa, *et al* [21]. While no significant changes in the majority of copper responsive genes were noted, most outside the *cso* (n = 18) were down regulated, short of our cutoff values. These include another copper sensing regulator, *ricR* (-1.5, FDR = 0.18). Among the RicR regulon [21], two genes, Rv0847 and Rv0848, were significantly repressed. Additionally, several of the other genes under the control of RicR (n = 7), including *mymT* a copper binding metallothionein [22] and *mmcO*, a multicopper oxidase which is exported across the cytoplasmic membrane [23], were slightly, though not significantly down regulated (Fig 4A), and this trend was also confirmed by qRT-PCR. These results clearly demonstrate that the CsoR and RicR regulons are distinct; however deregulation of the CsoR regulon may contribute to a slight, perhaps compensatory, increase in repression of the RicR regulon.

With evidence that CsoR directly regulates only its own operon, it seemed likely that other forms of regulation were at play in the Δ*csoR* strain. While no sigma factors were found to be differentially expressed, numerous transcriptional regulators were among those differentially expressed (n = 16) (Table 1). Therefore, the genes under transcriptional control of these regulators may represent a significant portion of the differentially expressed genes in our dataset.
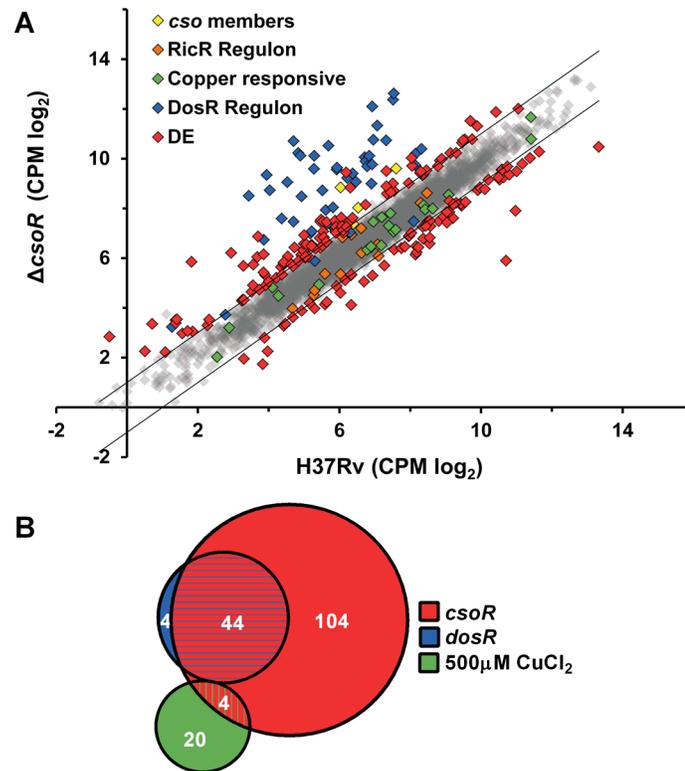
Fig 4. Analysis of the Δ*csoR* transcriptome. (A) Counts per million (CPM) of each gene detected in our RNA-Seq study, plotted for *M. tuberculosis* Δ*csoR* versus H37Rv wild type. Highlighted are members of the *cso* (yellow), members of the RicR regulon (orange), genes responsive to copper, but not part of the *cso* or RicR regulon (green), members of the DosR regulon (blue), and significantly differentially expressed genes as determined by an FDR $\geq$ 0.05 not included in the above groups (red). Two parallel, black lines demarcate the region outside of which differential expression values exceed our cutoff of a 2.0 fold difference between strains. Genes not meeting both cutoff values are shown as semi-transparent grey diamonds. Data points show the mean of two biological replicates. **(B)** Overlap of the induced *csoR* regulon (red) with 500 CuCl$_2$ inducible genes (green) and genes induced under the control of *dosR* (blue). Of the 152 genes induced in the Δ*csoR* strain compared to H37Rv wild type, only 4 overlapped with the 24 genes induced in H37Rv wild type when exposed to copper stress at 500µM CuCl$_2$. DosR inducible genes showed substantial overlap with Δ*csoR* with 44 out of 48 overlapping. The diagram is area-proportional.

One striking pattern was the induction of 44 out of 48 members of the *dosR* regulon, known for its role in response to hypoxia, nitric oxide, and dormancy [24, 25] (Fig 4B). These members of the *dosR* regulon were among the most highly induced genes in our dataset (Fig 4A). Another notable regulator involved in broad regulation of genes throughout various stages of hypoxia, Rv0081, was also induced [26]. This again suggests that *csoR* itself may not be directly controlling the expression of these genes, but rather derepression of its own regulon may be creating hypoxia-like stress conditions to which *dosR*, Rv0081, and other transcriptional regulators respond. Overall, our analyses suggest that CsoR represses its own operon, and absence of *csoR* may lead to a disruption in copper homeostasis, leading to a hypoxia or NO type stress response.

The impact of CsoR on drug resistance

During analysis of the *csoR* impacted genes it was noted that genes involved in the response to isoniazid (INH) were enriched, with 7 of the 23 known responders being induced. These 7 genes included several genes involved in fatty acid synthesis as well as membrane efflux protein, *efpA* (Table 1). Based on this finding and a previous study that showed the absence of *M*.

Table 1. Selected genes differentially expressed in *M. tuberculosis* ΔcsoR as compared to wild type.

Locus	Name	Description	Fold Change[a]	FDR[b]
Copper Responsive Genes				
Rv0848	cysK2	cysteine synthase A	-2.23	4.79E-04
Rv0967	csoR	copper-sensing transcriptional repressor	6.43	9.11E-22
Rv0968		conserved hypothetical protein	2.92	2.61E-09
Rv0969	ctpV	metal cation transporting P-type ATPase	4.11	3.51E-19
Rv0970		conserved membrane protein	1.96	8.89E-05
Transcriptional Regulators				
Rv0081		transcriptional regulator	6.99	2.46E-28
Rv0144		transcriptional regulator, tetR-family	-2.28	2.67E-06
Rv0386		transcriptional regulator, luxR/uhpA-family	2.42	4.60E-07
Rv0452		transcriptional regulator	2.31	1.30E-05
Rv0981	mprA	mycobacterial persistence regulator	-2.16	4.05E-06
Rv1129c		transcriptional regulator	-7.85	1.53E-07
Rv1657	argR	arginine repressor argR	-2.83	7.33E-09
Rv1985c		transcriptional regulator, lysR-family	-1.98	5.34E-04
Rv2017		transcriptional regulator	2.19	3.97E-06
Rv2621c		transcriptional regulator	2.59	2.23E-04
Rv2779c		transcriptional regulator, lrp/asnC-family	-3.02	8.11E-12
Rv3132c	dosS	two component system sensor histidine kinase	4.38	2.74E-22
Rv3133c	dosR	two component system transcriptional regulator	7.69	9.09E-37
Rv3197A	whiB7	transcriptional regulator whiB-like	-2.00	3.50E-04
Rv3334		transcriptional regulator, merR-family	2.94	4.37E-10
Rv3855	ethR	tetR-family transcriptional repressor	2.09	1.34E-03
INH Responsive Genes				
Rv1592c		conserved hypothetical protein	4.51	4.63E-23
Rv1854c	ndh	NADH dehydrogenase	2.09	2.27E-04
Rv2243	fabD	malonyl CoA-acyl carrier protein transacylase	3.42	4.10E-12
Rv2245	kasA	3-oxoacyl-[acyl-carrier protein] synthase 1	2.96	2.92E-09
Rv2247	accD6	acetyl/propionyl-CoA carboxylase beta subunit	2.16	4.42E-05
Rv2482	plsB2	glycerol-3-phosphate acyltransferase	-2.08	5.08E-06
Rv2846c	efpA	membrane efflux protein	2.35	8.54E-06

[a] Fold change in the ΔcsoR transcriptome as compared to wild type.

[b] As determined by Benjamini and Hochberg's algorithm

doi:10.1371/journal.pone.0151816.t001

smegmatis copper-responsive regulator GfcR increased INH resistance [27], we decided to investigate this phenotype in our mutant strain. Disc and MABA assays [19] examining inhibition of *M. tuberculosis* H37Rv and *ΔcsoR* growth revealed a slight but not significant difference in INH susceptibility between strains (S6 Fig). It may be that the induced INH responsive genes are responsive to more general stress conditions, and therefore are not those most relevant for mitigating INH related stress.

Expression dynamics of the copper sensing operon in the absence of *csoR* during copper stress

While we have shown that the *cso* is induced in the absence of *csoR* and copper stress, it is still unclear if CsoR deregulation alone accounts for the induction of the *cso* under copper stress.

To better examine the dynamics of CsoR regulation of the *cso* during copper stress, we utilized qRT-PCR to profile the expression levels of *csoR*, Rv0968, *ctpV*, and Rv0970. Samples for analysis were taken from *M. tuberculosis* H37Rv, *ΔcsoR*, and *ΔcsoR::csoR* left untreated or exposed to either 50 or 500μM $CuCl_2$ for 3 hours. As expected, qRT-PCR analysis of all 4 *cso* genes showed induction of the operon in the absence of *csoR* (Fig 5A). This level of induction was on par with the induction of the operon under moderate copper stress (50μM $CuCl_2$) in the wild type strain, but was less than the expression levels seen in wild type under high copper stress (500μM $CuCl_2$). Expression levels of the complement strain were similar to that of the knock-out. Interestingly, as the level of copper stress increased for the *ΔcsoR* strain, no change in *cso* expression was seen at 50 or 500μM $CuCl_2$ compared to untreated *ΔcsoR*, unlike in wild type (Fig 5B). Analysis of *ΔcsoR::csoR* on the other hand did reveal a modest rescue of the copper responsive phenotype.

To test the hypothesis that the *cso* may be under the control of multiple copper sensitive regulators and may not be responding to copper stress in *ΔcsoR* due to increased copper export, we sought to investigate the levels of copper present within each strain. Direct measures of copper such as neutron activation analysis are not reliably precise enough to detect small differences in copper ions within *M. tuberculosis* [15, 21]. Therefore *mmcO*, part of the copper responsive RicR regulon, was picked as an indirect indicator of copper stress experienced by the cell [18]. Thus, samples of wild type, *ΔcsoR*, and complement strains under different levels of copper stress were examined by qRT-PCR analysis for *mmcO*. No significant difference in *mmcO* induction was detected between strains (Fig 5C). As with the global transcriptome analysis, *mmcO* was slightly down-regulated in *ΔcsoR* as compared to wild type in copper-free media. This could be indicative of reduced levels of copper present in the *M. tuberculosis* cytoplasm in *ΔcsoR* in the absence of copper stress. However, once copper was added, *mmcO*, unlike the *cso*, increased drastically in the mutant strain. A similar profile was also observed when copper responsive gene *mymT* was analyzed (S7 Fig). These results indicated that under copper stress, copper levels between the three strains were equivalent, excluding the possibility that differences in intracellular copper were contributing to the differential expression of the *cso*. We cannot, however, rule out the possibility that other regulators, responsive to copper or related stress, participate in the regulation of the *cso*.

Discussion

Recently, great interest has been taken in the importance of copper homeostasis and its role in bacterial pathogenesis and host defense [28]. Previously, our group elucidated the regulatory mechanisms behind the copper responsive transcriptional repressor CsoR [13]. We have also shown the shuttling activity of one of its directly regulated genes, *ctpV*, in response to copper stress [15]. In this study, we examined the importance of this negative regulator, CsoR, to both copper and host-mediated stress in a murine model of tuberculosis. While a multifaceted role of CsoR had been previously suggested—in which CsoR has a buffering effect preventing damage from free copper [13]—our results suggest that the genes within the CsoR regulon, rather than CsoR itself, are primarily responsible for directly mitigating the harmful effects of copper stress. Consistent with this hypothesis, the survival curves of *ΔcsoR* at 500μm $CuCl_2$ are reminiscent of those seen for *M. tuberculosis ΔctpV::ctpV*, which overexpresses *ctpV*, a copper exporting member of the *csoR* regulon [15]. Less expected was the dramatic difference in strain survival depending on the use of a fresh, log stage inoculum or one that had been grown to stationary phase before inoculation in copper containing media. One possible cause of this difference could be a slower response to copper stress in the stationary phase cultures, exaggerating the otherwise slight copper resistant phenotype of *ΔcsoR*. On the other hand, it may be that the
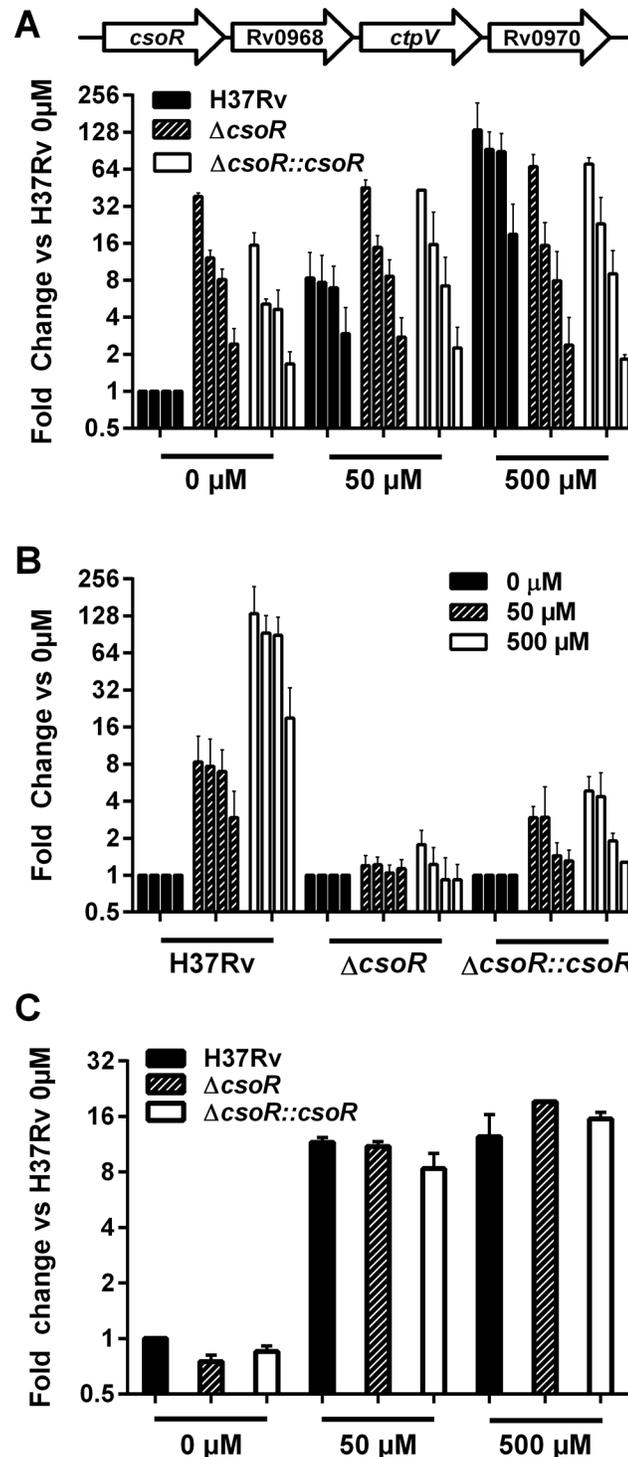
Fig 5. Expression of *cso* genes during copper stress in the absence of *csoR*. qRT-PCR was used to analyze expression levels of *csoR*, Rv0968, *ctpV*, and Rv0970. A schematic of the operon (not drawn to scale) is shown above the graph and the order of the genes in the operon corresponds to the order in which expression levels are graphed for each gene. **(A)** *M. tuberculosis* strains H37Rv (black), Δ*csoR* (striped), or Δ*csoR*::*csoR* (white) were exposed to CuCl$_2$ at 50 or 500µM or left untreated (0µM) for 3 hours. Values shown are the mean fold change between each gene and its untreated wild type counterpart after normalization to *sigA* expression levels. **(B)** A second comparison of the same samples was done showing the mean fold change between each gene after normalization to *sigA* expression levels at 50µM (striped) or

500µM (white) and its untreated counterpart (black) from the same strain. Data represent one of two similar biological replicates. Error bars represent the standard error of the mean from three technical replicates. **(C)** Expression levels of *mmcO* as determined by qRT-PCR analysis of the same samples–H37Rv (black), Δ*csoR* (striped), or Δ*csoR*::*csoR* (white)–left untreated (0µM) or stressed with 50µM or 500µM CuCl$_2$. Fold change is shown as expression levels of each gene relative to expression levels in untreated wild type culture after normalization to *sigA* expression levels. Data represent one of two similar biological replicates. Error bars represent the standard error of the mean from two technical replicates.

cso has a more important role to play during dormancy than during logarithmic phase growth, particularly after lengthy exposures to copper that may allow copper to build up within the cell.

The role of the *cso* in dormancy is supported by the observed induction of *csoR* throughout the enduring hypoxic response [29]. An increased, hypoxia-specific copper response may be physiologically important as not only is copper more toxic under hypoxic conditions [30], but hypoxia stimulates macrophages to increase copper uptake [31]. In fact hypoxia and high copper levels have both been found within granulomas of guinea pigs during *M. tuberculosis* infection, emphasizing the need to adapt to combat both stress conditions simultaneously [4, 32]. At the same time, the *M. tuberculosis* requirement for copper under hypoxia is decreased as copper-independent cytochrome *bd* oxidase is induced, reducing the need for copper-dependent cytochrome *c* oxidase [12]. The relationship of *csoR*, copper stress, and hypoxia-induced dormancy is currently being investigated further.

As the host environment [32], particularly the mycobacterial phagosome [5] is known to harbor high levels of copper during *M. tuberculosis* infection as a potential antimicrobial defense mechanism, we were interested in testing if the increased resistance to copper of the Δ*csoR* strain translated to our murine aerosol infection model. Mouse infections revealed that despite similar CFU counts at week 2, the mutant strain multiplied and survived nearly a log fold above wild type through the early stages of chronic infection at weeks 4 and 8. These results might be attributed to the preparedness of the Δ*csoR* strain to face host stress conditions even before they were detected; as transcriptional analysis indicated, the mutant strain already had genes induced that typically respond specifically to host stressors such as copper (*ctpV*), nitric oxide, and hypoxia (*dosR* regulon). Toxic copper levels and nitric oxide are stressors faced by *M. tuberculosis* within the phagosome of macrophages, especially those that have been activated. This activation follows the initiation of the adaptive immune response to *M. tuberculosis* infection taking place around weeks 2 to 4 [33], after which the Δ*csoR* strain shows improved survival over wild type. Previously published data examining our Δ*cso* strain demonstrated a phenotype opposite of that observed for Δ*csoR* during mouse infection [34]. Unlike our Δ*csoR* strain, where the remaining members of the *cso* are induced, the Δ*cso* strain was attenuated, particularly during the later time points of chronic infection [34]. This earlier study, and our transcriptional study showing the induction of the cso during mouse infection [35], highlight the importance of the whole *cso* operon to the survival of *M. tuberculosis* during infection.

To better understand the control CsoR has over its own operon, we studied transcriptional expression of the *cso* in wild type, knockout, and complement strains in untreated culture and under two levels of copper (50, and 500µM). As expected, we found that without *csoR*, the *cso* genes were induced in the absence of copper. Notably, this induction is not to the same level as the induction seen in wild type under high levels of copper stress (500µM). This indicates that at high levels of copper, CsoR derepression may not be solely responsible for *cso* induction. This hypothesis is consistent with the idea that genes outside of the core copper responsive regulon (n = 15 induced at 50µM CuCl$_2$) are induced to address secondary stress such as the presence of reactive oxygen and nitrogen species at higher copper levels (n = 30 induced at 500µM

CuCl$_2$) [6]. It could be that a second transcriptional regulator is required to further induce the *cso* in response to this toxic level of copper stress. Therefore, disruption of sequence near the binding site of a second regulator may have contributed to a lesser level of *cso* induction. One such candidate may be transcriptional regulator Rv2324 predicted to bind within *csoR* just upstream of the deletion site [26]. Therefore, the attenuated *cso* induction under high levels of copper stress may have attributed to a more modest survival phenotype of the Δ*csoR* strain under copper and host stress than might otherwise be expected.

Despite the apparent advantage of losing *csoR* under both copper and host stress, our global transcriptional analysis reveals the important role *csoR* plays in the cell under normal growth conditions. While this work has not ventured to define the direct targets of CsoR regulation, our results support previous findings that CsoR may only regulate its own operon [21]. Both studies found the other members of the *cso* to be induced in the *csoR* mutants to similar levels. The previous study [21], however, found no differentially expressed genes outside of the *cso*, in stark contrast to our list of 223 differentially regulated genes. It is possible, as the authors point out, that the previously studied strain is a polar knockout, unlike ours. It may be that translation of the *cso* in their Δ*csoR*:: *hyg*$_R$ strain was not as efficient as in the Δ*csoR* strain discussed here, therefore mitigating any stress we posit is placed on the cell when the operon is deregulated in the absence of *csoR*. We hypothesize that this stress is derived from the consequences of *cso* overexpression in the absence of copper. Interestingly, outside of the *cso*, the only copper responsive genes to be differentially expressed were down regulated [6]. It may be that lower levels of copper in the Δ*csoR* strain, due to increased Cu export by CtpV, tightened copper mediated repression of these genes such as *mmcO* and *mymT*, by regulators such as RicR. This tightening of repression was observed in our RNA-Seq and confirmed by qRT-PCR above. This compensatory response suggests a hierarchy of copper regulation in *M. tuberculosis* with CsoR having a key role. It should also be noted, however, that these previous studies were conducted using microarray analysis, which can be less sensitive to differential expression than RNA-Seq analysis [36]. Therefore, the absence of more extensive overlap among these studies may be partially due to the difference in technique used.

A major consequence of the loss of *csoR* and the deregulation of the *cso* was the induction of the DosR regulon. While culture manipulation can cause a slight but significant induction of the DosR regulon [37], great care was taken to quickly process all samples to be used for RNA analysis in an identical fashion. The observed induction of the DosR regulon was substantial, and likely too high to be caused by handling differences. While the mechanism for this induction remains unresolved, we have modeled two opposing hypotheses (Fig 6). The first is based on data suggesting that disruption in the electron transport system or cytochrome c oxidase induces expression of the DosR regulon [25, 38] (Fig 6A). As cytochrome c oxidase, involved in the terminal steps of cellular respiration, is a copper metalloenzyme, *cso* induction resulting in excessive copper export could negatively impact its function. This block in respiration may contribute to the activation of the DosR regulon.

A second possibility could be that NO is directly inducing the DosR regulon in our Δ*csoR* strain (Fig 6B). While we hypothesize that copper may be present at lower levels in the cytoplasmic space, CtpV is thought to export copper across only the cell membrane. We do not know if expression levels of genes involved in the export of copper across the mycobacterial cell wall were affected, as the only gene proposed to fulfill this role in *M. tuberculosis*, Rv1698, was later excluded as a potential candidate [32, 40]. Thus it is possible that copper could be accumulating and causing damage in the mycobacterial periplasmic space of Δ*csoR*. This damage could be exacerbated by the slight down-regulation of a recently characterized periplasmic multicopper oxidase, *mmcO* [23]. Cu(I) can generate NO through interactions with S-nitrosothiols [39], which could subsequently induce the DosR regulon.
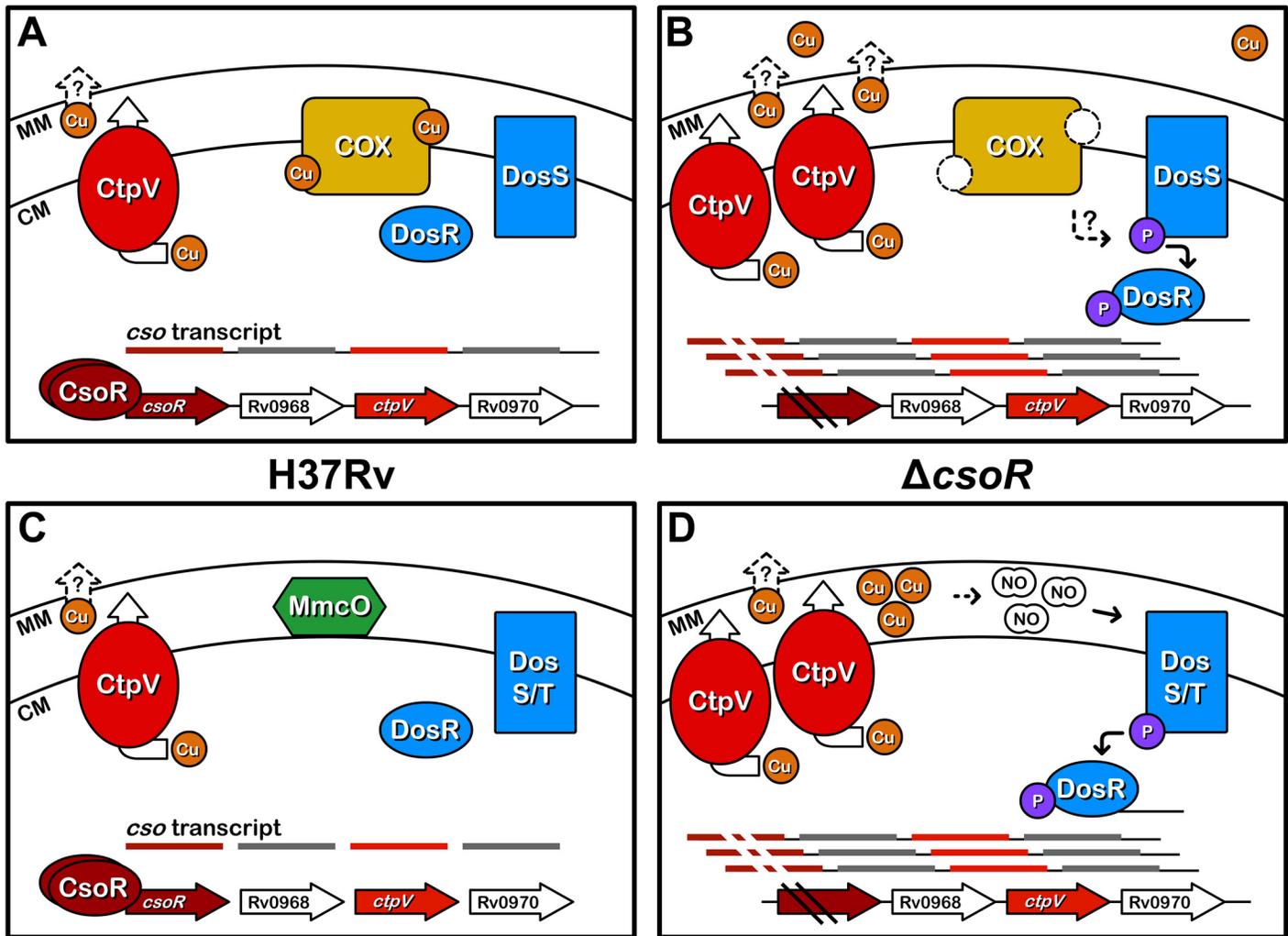
Fig 6. Potential consequences of Δ*csoR* disrupted copper homeostasis. Overexpression of the *cso* and the proteins it codes for after deletion of *csoR* (dark red) may result in excessive levels of copper export by CtpV (red). **(A)** As a result, pools of copper (orange) for metalloenzyme usage may be depleted, reducing the levels of functional proteins such as cytochrome c oxidase (yellow), as seen in the panel on the right. This could potentially slow the electron transport chain leading to the induction of the DosR (blue) regulon through the redox sensor, DosS (blue) [38]. The wild type strain is shown in the panel on the left for comparison. **(B)** Alternatively, the increased cytoplasmic export of copper may lead to a buildup of copper in the mycobacterial periplasmic space where MmcO (green) usually assists in copper detoxification. The increased copper stress in this region may be magnified, however, by the down regulation of *mmcO* in the mutant strain. Free copper can lead to the production of reactive nitrogen species, such as NO [39]. NO can trigger expression of the DosR regulon [25]. The wild type strain is shown in the panel on the left for comparison. CM; cytoplasmic membrane. MM; mycomembrane. Cu; copper. NO; nitric oxide. COX; cytochrome c oxidase. P; phosphoryl group.

doi:10.1371/journal.pone.0151816.g006

These scenarios and the stressed transcriptional profile of the Δ*csoR* strain highlight the potential harm that can be done even at low levels of copper and emphasize the need for balance in regulating the level of intracellular copper, as aided by *csoR*. This increased understanding of the balance of copper *M. tuberculosis* must maintain during infection may ultimately help guide development of antimycobacterial therapies that wish to utilize copper or target the copper stress response. Overall this study has revealed new insights into the importance of copper regulation and *csoR*, not only under copper stress, but also in its absence. Similar copper regulators are present in other intracellular pathogens and similar scenarios could be at play in these organisms as well.

Materials and Methods

Strain construction

Strains used in this work include *Mycobacterium tuberculosis* H37Rv, and its derivatives *M. tuberculosis* ΔcsoR and *M. tuberculosis* ΔcsoR::csoR. To create an inactivating mutation in *csoR* in *M. tuberculosis*, we first generated a ΔcsoR::hyg_R strain using specialized transduction and homologous recombination as outlined previously [14, 34] and confirmed by sequencing and Southern blot [34]. To determine the polar or nonpolar nature of the construct, RNA was isolated from the strain using a TRIzol® Reagent based method before treatment with TURBO™ DNase (Ambion®, Austin, TX) until PCR negative. RNA was then reverse transcribed to cDNA using Superscript® III (Invitrogen, Carlsbad, CA). cDNA was then screened by PCR for the expression of the genes downstream of *csoR*: Rv0968, *ctpV*, and Rv0970. Our analysis indicated that the mutant was polar.

To construct an unmarked mutant strain, a helper plasmid, pYUB870, was used to remove the hyg_R gene as described previously [14], leaving behind a stop codon at the 14th amino acid of the *csoR* gene. Again these results were confirmed by sequencing and the nonpolar nature of this mutant was demonstrated as described above. This strain was used for the construction of a complement strain. The *csoR* gene and the 200bp promoter region upstream of the *csoR* transcriptional start site were cloned into the integrative, *E. coli*-mycobacterial shuttle vector pMV306, originally derived from pMV361 [41]. The vector, containing a kanamycin resistance marker, was electroporated into *M. tuberculosis* ΔcsoR. Successful electroporants were identified by screening colonies growing on Middlebrook 7H10 media supplemented with 10% ADC and 30 μg/ml kanamycin by PCR targeting *csoR* and the upstream portion of the pMV306 vector. The final clone was verified by sequencing.

Growth conditions

Starter cultures for experiments were grown from frozen stocks in liquid media to late log stage (~OD_{600} 1.0) in Middlebrook 7H9 (Remel™, Lenexa, KS) with 10% ADC and 0.05% TWEEN 80. For all experiments, 30μg/ml kanamycin were included in growth media used for *M. tuberculosis* ΔcsoR::csoR. Before use in downstream experiments, bacteria taken from 7H9 cultures were washed twice with copper-free Sauton's media. Similarly, all reagents and media used in copper sensitive experiments were treated with 0.2% (w/v) Chelex® 100 (Sigma-Aldrich, St. Louis, MO) to remove traces of copper prior to addition of other metal supplements before use. All glassware was acid washed with 1M nitric acid to remove any traces of metal ions. For transcriptional experiments, washed *M. tuberculosis* strains H37Rv, ΔcsoR, and ΔcsoR::csoR were inoculated to an OD_{600} of 0.10 in 30 or 100 ml Sauton's media containing 0.05% TWEEN 80. At late log phase (~OD_{600} 1.0) cultures were exposed to untreated media or 50 or 500μM $CuCl_2$ for 3 hours before collecting cultures for RNA extraction as detailed previously [6].

Microplate Alamar Blue Assay (MABA)

To quantify the level of resistance of *M. tuberculosis* constructs to copper, MABA assays were performed as described previously [18, 19] with a few modifications. Briefly, the outer wells of flat bottom 96-well microplates were filled with sterile ddH_2O to prevent evaporation. Inner wells were filled with 100ul Sauton's broth containing serial dilutions of $CuCl_2$ in duplicate or no added $CuCl_2$ as a control and *M. tuberculosis* strains H37Rv, ΔcsoR, and ΔcsoR::csoR inoculated to a theoretical OD_{600} of 0.05. A series of nine, two-fold dilutions were made with $CuCl_2$ from 16 to 4000μM. On day 5 after inoculation, 30μl Alamar Blue (Invitrogen; Carlsbad, CA): TWEEN 80 (1:1) were added to a control well and incubated an additional 24hrs. When a shift

in color from blue to pink was seen on the following day, 30µl Alamar blue:TWEEN 80 (1:1) was added to each of the remaining wells. Data were collected the following day and the blue wells containing the lowest concentration of CuCl$_2$ were recorded for each series and each strain as the minimum inhibitory concentration (MIC).

Mouse infections

BALB/c mice (Harlan, Indianapolis, IN) were infected with *M. tuberculosis* H37Rv wild type or Δ*csoR* strains using an aerosol infection model with the Glas-Col® Inhalation Exposure System (Glas-Col, LLC, Terre Haute, IN) as outlined before [15]. At 2, 4, 8, and 25 weeks groups of 3 to 5 mice were euthanized by cervical dislocation following anesthetization by isoflurane, and lung, spleen, and liver were collected for colony counts and histopathology [15]. Aside from the 25 week time point, the experiment was completed in duplicate.

Ethics statement

Animal experiments were approved by the Institutional Animal Care and Use Committee, University of Wisconsin-Madison (V1095) in compliance with the regulations set in place by the Public Health Service Policy on the Humane Care and Use of Laboratory Animals, overseen by the NIH Office of Laboratory Animal Welfare (OLAW). Mice were monitored daily by caretakers for signs of illness or distress and all efforts were taken to prevent animal suffering. No unexpected deaths occurred during the study and all mice reached predetermined endpoints without showing signs such as behavioral changes, fur ruffling, anorexia, or lethargy that would require the use of a humane endpoint.

Quantitative, real-time PCR

RNA was isolated for qRT-PCR immediately after collecting the cultures using a TRIzol based method described previously [15, 34]. RNA was treated with TURBO DNase until PCR negative to remove contaminating DNA. For qRT-PCR analysis of the *cso*, 1–2µg RNA were used as template for cDNA using Superscript III. A SYBR green based qRT-PCR protocol utilizing GoTaq® qPCR Master Mix (Promega, Madison, WI) and the StepOnePlus™ Real-Time PCR System (Applied Biosystems®, Foster City, CA) were used. Expression of all genes was normalized to *sigA* expression levels. Analysis was carried out using LinRegPCR [42]. Two biological replicates with no less than two technical replicates each were completed.

Transcriptional profiling through RNA sequencing

For transcriptional profiling with RNA-Seq technology, RNA was isolated from cultures grown in Sauton's broth to late log phase and treated with TURBO DNAse as done with samples for qRT-PCR. RNA integrity was confirmed using the 2100 Bioanalyzer (Agilent, Santa Clara, CA). The 23S, 16S, and 5S rRNAs were depleted from the samples using the Ribo-Zero™ Magnetic Kit for bacteria (Epicentre, Madison, WI). Biological replicates of prepared rRNA-reduced RNA were submitted to the University of Wisconsin Biotechnology Center's DNA Sequencing Facility where they were prepared for sequencing using the TruSeq RNA Sample Preparation Kit (Illumina®, San Diego, CA). The samples were run on an Illumina HiSeq™ 2000 to generate 100bp single reads. Base calling was done in CASAVA 1.8.2. Before differential expression analysis the quality of the FASTQ files was checked using the FASTX-Toolkit developed in the lab of Gregory Hannon at Cold Spring Harbor (http://hannonlab.cshl.edu/fastx_toolkit/index.html). Sequence reads were mapped to the *M. tuberculosis* H37Rv genome using Bowtie [43]. Reads mapping to more than one location within the genome were excluded

from further analysis. BEDTools was used to determine counts for each coding sequence in the *M. tuberculosis* H37Rv genome [44]. The above analyses were carried out within the web-based Galaxy platform [45, 46, 47]. Differential expression analysis using the output count data was carried out in R with the Bioconductor software package, edgeR [48]. Genes demonstrating ≥ 2 fold differential expression between $\Delta csoR$ and wild type strains, and having an FDR < 0.05 were considered to be differentially expressed. Confirmation of 10 differentially expressed genes was carried out by qRT-PCR as detailed above.

Whole genome sequencing

Genomic DNA was extracted as described previously [49]. Quality was confirmed by gel electrophoresis and measuring absorbance at 260nm and 280nm. Samples were submitted to the University of Wisconsin Biotechnology Center's DNA Sequencing Facility where they were prepared for sequencing using the NEBNext® Ultra™ DNA Library Prep Kit for Illumina® (New England Biolabs, Ipswich, MA). The samples were run on an Illumina MiSeq™ to generating 300bp paired end reads. Base calling was done in CASAVA 1.8.2. Reads were mapped to the *M. tuberculosis* H37Rv genome (NC_000962.3) using the CLC Genomics Workbench 8.0.1 (CLC bio, Aarhus, Denmark). SNPs were detected using the Fixed Ploidy Variant Detection tool, and larger genomic variations were detected using the InDels and Structural Variants tool with the same software.

Statistical analysis

For large scale differential expression analysis, false discovery rates were calculated using the Benjamini and Hochberg algorithm [50] with a cutoff for significance at FDR < 0.05. For all other experiments, statistical significance was determined using Student's *t*-test with cutoff value of $P < 0.05$.

Supporting Information

S1 Fig. Growth kinetics of $\Delta csoR$ under copper stress. Growth of *M. tuberculosis* H37Rv (circles) and $\Delta csoR$ (squares) over the course of 15 days in Sauton's media left with 50μM CuCl$_2$ from **(A)** log stage or **(B)** stationary stage inocula. Shown are one of two similar biological replicates with error bars representing standard deviation.
(TIF)

S2 Fig. Growth inhibition of wild type H37Rv, $\Delta csoR$, and complement strains by CuCl$_2$. *M. tuberculosis* H37Rv (red circles), $\Delta csoR$ (green squares), and complement (blue triangles) strains were exposed to two-fold dilutions of CuCl$_2$ in Sauton's broth from 16μM to 4000μM. Percent reduction of Alamar blue reagent as compared to untreated wells was used to measure growth. Data are representative of two biological replicates.
(TIF)

S3 Fig. Growth of $\Delta csoR$ and wild type H37Rv in the spleen and liver during mouse infection. Groups of BALB/c mice were infected by aerosol route with either *M. tuberculosis* H37Rv (filled circles) or $\Delta csoR$ (open squares). Shown are CFU/g of **(A)** spleen or **(B)** liver for individual mice over the course of 25 weeks representative of one of two similar experiments. Dashed lines indicate the limit of detection (500 and 100 CFU/g respectively) for each experiment. Data and mean shown are composites from two independent experiments. **(C)** Total grams body weight were also recorded and represent a single experiment. *P = 0.005.
(TIF)

S4 Fig. Histopathology scores of wild type and Δ*csoR* in the lung, spleen, and liver during mouse infection. Groups of BALB/c mice were infected by aerosol route with either *M. tuberculosis* H37Rv (filled circles) or Δ*csoR* (open squares). Shown are histopathology scores (0, absent; 1, minimal; 2, mild; 3, moderate; 4, severe; 5, massive) for **(A)** granulomatous inflammation and **(B)** bronchiole-associated lymphoid tissue in the lungs; **(C)** granulomatous inflammation and **(D)** lymphocytic inflammation in the liver; and **(E)** granulomatous inflammation and **(F)** follicular atrophy in the spleen. Data represent all readings for three animals per time point in each group.
(TIF)

S5 Fig. RT-PCR confirmation of RNA-Seq results. qRT-PCR was used to confirm the differential expression of 10 genes, 6 induced and 4 repressed, identified from the RNA-Seq experiment. Shown is the fold change of gene expression in the Δ*csoR* strain compared to wild type for the RNA-Seq data (black) and the qRT-PCR confirmation (white). For qRT-PCR data, the means of two biological replicates are shown with error bars representing the standard deviations.
(TIF)

S6 Fig. Isoniazid resistance in Δ*csoR*. (A) 6mm discs were impregnated with 160ng isoniazid and placed on 7H10 agar plates with ADC spread with 100ul late log stage culture of *M. tuberculosis* H37Rv (red) or Δ*csoR* (green). Once a lawn of growth was detected, the radius of the zone of inhibition around the disc was measured. Error bars indicate the standard deviation. Data are representative of two biological replicates. **(B)** *M. tuberculosis* H37Rv (red circles) and Δ*csoR* (green squares) were exposed to two-fold dilutions of isoniazid in 7H9 broth with ADC from 3ng/ml to 80ng/ml. Percent reduction of Alamar blue reagent as compared to untreated wells was used to measure growth. Data are representative of two biological replicates.
(TIF)

S7 Fig. Assessing copper levels in the cell using *mymT* transcription levels as an indirect indicator. Expression levels of *mymT* as determined by qRT-PCR analysis of samples H37Rv, Δ*csoR*, or Δ*csoR*::*csoR* left untreated (0μM) (black) or stressed with 50μM (striped) or 500μM (white) CuCl$_2$. Fold change is shown as expression levels of each gene relative to expression levels in untreated wild type culture after normalization to *sigA* expression levels. Data represent one of two similar biological replicates. Error bars represent the standard error of the mean from two technical replicates.
(TIF)

S1 Table. Total RNA-Seq reads mapping to the M. tuberculosis H37Rv genome.
(XLSX)

S2 Table. All significantly differentially expressed genes in *M. tuberculosis* Δ*csoR* as compared to H37Rv wild type.
(XLSX)

Acknowledgments

Author Contributions

Conceived and designed the experiments: SAM AMT. Performed the experiments: SAM SWS. Analyzed the data: SAM SWS HS AMT. Contributed reagents/materials/analysis tools: SAM AMT. Wrote the paper: SAM AMT.

References

1. World Health Organization (WHO). Global tuberculosis report 2013. Geneva: WHO; 2013 Oct 23.

2. Adams LB, Dinauer MC, Morgenstern DE, Krahenbuhl JL. Comparison of the roles of reactive oxygen and nitrogen intermediates in the host response to *Mycobacterium tuberculosis* using transgenic mice. Tuber Lung Dis 1997; 78: 237–246. PMID: 10209678

3. Schaible UE, Sturgill-Koszycki S, Schlesinger PH, Russell DG. Cytokine activation leads to acidification and increases maturation of *Mycobacterium avium*-containing phagosomes in murine macrophages. J Immunol 1998; 160: 1290–1296. PMID: 9570546

4. Via LE, Lin PL, Ray SM, Carrillo J, Allen SS, Eum SY, et al. Tuberculous granulomas are hypoxic in guinea pigs, rabbits, and nonhuman primates. Infect Immun 2008; 76: 2333–2340. doi: 10.1128/IAI. 01515-07 PMID: 18347040

5. Wagner D, Maser J, Lai B, Cai Z, Barry CE III, Honer Zu BK, et al. Elemental analysis of *Mycobacterium avium*-, *Mycobacterium tuberculosis*-, and *Mycobacterium smegmatis*-containing phagosomes indicates pathogen-induced microenvironments within the host cell's endosomal system. J Immunol 2005; 174: 1491–1500. PMID: 15661908

6. Ward SK, Hoye EA, Talaat AM. The global responses of *Mycobacterium tuberculosis* to physiological levels of copper. J Bacteriol 2008; 190: 2939–2946. doi: 10.1128/JB.01847-07 PMID: 18263720

7. Domek MJ, LeChevallier MW, Cameron SC, McFeters GA. Evidence for the role of copper in the injury process of coliform bacteria in drinking water. Appl Environ Microbiol 1984; 48: 289–293. PMID: 6385846

8. Wardman P, Candeias LP. Fenton chemistry: an introduction. Radiat Res 1996; 145: 523–531. PMID: 8619017

9. Macomber L, Imlay JA. The iron-sulfur clusters of dehydratases are primary intracellular targets of copper toxicity. Proc Natl Acad Sci U S A 2009; 106: 8344–8349. doi: 10.1073/pnas.0812808106 PMID: 19416816

10. Arredondo M, Nunez MT. Iron and copper metabolism. Mol Aspects Med 2005; 26: 313–327. PMID: 16112186

11. Spagnolo L, Toro I, D'Orazio M, O'Neill P, Pedersen JZ, Carugo O, et al. Unique features of the *sodC*-encoded superoxide dismutase from *Mycobacterium tuberculosis*, a fully functional copper-containing enzyme lacking zinc in the active site. J Biol Chem 2004; 279: 33447–33455. PMID: 15155722

12. Neyrolles O, Wolschendorf F, Mitra A, Niederweis M. Mycobacteria, metals, and the macrophage. Immunol Rev 2015; 264: 249–263. doi: 10.1111/imr.12265 PMID: 25703564

13. Liu T, Ramesh A, Ma Z, Ward SK, Zhang L, George GN, et al. CsoR is a novel *Mycobacterium tuberculosis* copper-sensing transcriptional regulator. Nat Chem Biol 2007; 3: 60–68. PMID: 17143269

14. Bardarov S, Bardarov S Jr, Pavelka MSJ Jr, Sambandamurthy V, Larsen M, Tufariello J, et al. Specialized transduction: an efficient method for generating marked and unmarked targeted gene disruptions in *Mycobacterium tuberculosis*, *M*. *bovis* BCG and *M*. *smegmatis*. Microbiology 2002; 148: 3007–3017. PMID: 12368434

15. Ward SK, Abomoelak B, Hoye EA, Steinberg H, Talaat AM. CtpV: a putative copper exporter required for full virulence of *Mycobacterium tuberculosis*. Mol Microbiol 2010; 77: 1096–1110. doi: 10.1111/j. 1365-2958.2010.07273.x PMID: 20624225

16. Cole ST, Brosch R, Parkhill J, Garnier T, Churcher C, Harris D, et al. Deciphering the biology of *Mycobacterium tuberculosis* from the complete genome sequence. Nature 1998; 393: 537–544. PMID: 9634230

17. Ioerger TR, Feng Y, Ganesula K, Chen X, Dobos KM, Fortune S, et al. Variation among genome sequences of H37Rv strains of *Mycobacterium tuberculosis* from multiple laboratories. J Bacteriol 2010; 192: 3645–3653. doi: 10.1128/JB.00166-10 PMID: 20472797

18. Speer A, Rowland JL, Haeili M, Niederweis M, Wolschendorf F. Porins Increase Copper Susceptibility of *Mycobacterium tuberculosis*. J Bacteriol 2013; 195: 5133–5140. doi: 10.1128/JB.00763-13 PMID: 24013632

19. Franzblau SG, Witzig RS, McLaughlin JC, Torres P, Madico G, Hernandez A, et al. Rapid, low-technology MIC determination with clinical *Mycobacterium tuberculosis* isolates by using the microplate Alamar Blue assay. J Clin Microbiol 1998; 36: 362–366. PMID: 9466742

20. Smaldone GT, Helmann JD. CsoR regulates the copper efflux operon *copZA* in *Bacillus subtilis*. Microbiology 2007; 153: 4123–4128. PMID: 18048925

21. Festa RA, Jones MB, Butler-Wu S, Sinsimer D, Gerads R, Bishai WR, et al. A novel copper-responsive regulon in *Mycobacterium tuberculosis*. Mol Microbiol 2011; 79: 133–148. doi: 10.1111/j.1365-2958.2010.07431.x PMID: 21166899

22. Gold B, Deng H, Bryk R, Vargas D, Eliezer D, Roberts J, et al. Identification of a copper-binding metallothionein in pathogenic mycobacteria. Nat Chem Biol 2008; 4: 609–616. doi: 10.1038/nchembio.109 PMID: 18724363

23. Rowland JL, Niederweis M. A multicopper oxidase is required for copper resistance in *Mycobacterium tuberculosis*. J Bacteriol 2013; 195: 3724–3733. doi: 10.1128/JB.00546-13 PMID: 23772064

24. Sherman DR, Voskuil M, Schnappinger D, Liao R, Harrell MI, Schoolnik GK. Regulation of the *Mycobacterium tuberculosis* hypoxic response gene encoding alpha -crystallin. Proc Natl Acad Sci U S A 2001; 98: 7534–7539. PMID: 11416222

25. Voskuil MI, Schnappinger D, Visconti KC, Harrell MI, Dolganov GM, Sherman DR, et al. Inhibition of respiration by nitric oxide induces a *Mycobacterium tuberculosis* dormancy program. J Exp Med 2003; 198: 705–713. PMID: 12953092

26. Galagan JE, Minch K, Peterson M, Lyubetskaya A, Azizi E, Sweet L, et al. The *Mycobacterium tuberculosis* regulatory network and hypoxia. Nature 2013; 499: 178–183. doi: 10.1038/nature12337 PMID: 23823726

27. Rao M, Liu H, Yang M, Zhao C, He ZG. A copper-responsive global repressor regulates expression of diverse membrane-associated transporters and bacterial drug resistance in mycobacteria. J Biol Chem 2012; 287: 39721–39731. doi: 10.1074/jbc.M112.383604 PMID: 23014988

28. Hodgkinson V, Petris MJ. Copper homeostasis at the host-pathogen interface. J Biol Chem 2012; 287: 13549–13555. doi: 10.1074/jbc.R111.316406 PMID: 22389498

29. Rustad TR, Harrell MI, Liao R, Sherman DR. The enduring hypoxic response of *Mycobacterium tuberculosis*. PLoS One 2008; 3: e1502. doi: 10.1371/journal.pone.0001502 PMID: 18231589

30. Beswick PH, Hall GH, Hook AJ, Little K, McBrien DC, Lott KA. Copper toxicity: evidence for the conversion of cupric to cuprous copper in vivo under anaerobic conditions. Chem Biol Interact 1976; 14: 347–356. PMID: 182394

31. White C, Kambe T, Fulcher YG, Sachdev SW, Bush AI, Fritsche K, et al. Copper transport into the secretory pathway is regulated by oxygen in macrophages. J Cell Sci 2009; 122: 1315–1321. doi: 10.1242/jcs.043216 PMID: 19351718

32. Wolschendorf F, Ackart D, Shrestha TB, Hascall-Dove L, Nolan S, Lamichhane G, et al. Copper resistance is essential for virulence of *Mycobacterium tuberculosis*. Proc Natl Acad Sci U S A 2011; 108: 1621–1626. doi: 10.1073/pnas.1009261108 PMID: 21205886

33. Flynn JL, Chan J. Immunology of tuberculosis. Annu Rev Immunol 2001; 19: 93–129. PMID: 11244032

34. Abomoelak B, Hoye EA, Chi J, Marcus SA, Laval F, Bannantine JP, et al. *mosR*, a novel transcriptional regulator of hypoxia and virulence in *Mycobacterium tuberculosis*. J Bacteriol 2009; 191: 5941–5952. doi: 10.1128/JB.00778-09 PMID: 19648248

35. Talaat AM, Lyons R, Howard ST, Johnston SA. The temporal expression profile of *Mycobacterium tuberculosis* infection in mice. Proc Natl Acad Sci U S A 2004; 101: 4602–4607. PMID: 15070764

36. Wang Z, Gerstein M, Snyder M. RNA-Seq: a revolutionary tool for transcriptomics. Nat Rev Genet 2009; 10: 57–63. doi: 10.1038/nrg2484 PMID: 19015660

37. Kendall SL, Movahedzadeh F, Rison SC, Wernisch L, Parish T, Duncan K, et al. The *Mycobacterium tuberculosis dosRS* two-component system is induced by multiple stresses. Tuberculosis (Edinb) 2004; 84: 247–255.

38. Honaker RW, Dhiman RK, Narayanasamy P, Crick DC, Voskuil MI. DosS responds to a reduced electron transport system to induce the *Mycobacterium tuberculosis* DosR regulon. J Bacteriol 2010; 192: 6447–6455. doi: 10.1128/JB.00978-10 PMID: 20952575

39. Dicks AP, Williams DL. Generation of nitric oxide from S-nitrosothiols using protein-bound Cu2+ sources. Chem Biol 1996; 3: 655–659. PMID: 8807899

40. Rowland JL, Niederweis M. Resistance mechanisms of *Mycobacterium tuberculosis* against phagosomal copper overload. Tuberculosis (Edinb) 2012; 92: 202–210.

41. Stover CK, de la Cruz VF, Fuerst TR, Burlein JE, Benson LA, Bennett LT, et al. New use of BCG for recombinant vaccines. Nature 1991; 351: 456–460. PMID: 1904554

42. Ruijter JM, Ramakers C, Hoogaars WM, Karlen Y, Bakker O, van den Hoff MJ, et al. Amplification efficiency: linking baseline and bias in the analysis of quantitative PCR data. Nucleic Acids Res 2009; 37: e45. doi: 10.1093/nar/gkp045 PMID: 19237396

43. Langmead B. Aligning short sequencing reads with Bowtie. Curr Protoc Bioinformatics 2010; 11.7: 1–14

44. Quinlan AR, Hall IM. BEDTools: a flexible suite of utilities for comparing genomic features. Bioinformatics 2010; 26: 841–842. doi: 10.1093/bioinformatics/btq033 PMID: 20110278

45. Goecks J, Nekrutenko A, Taylor J. Galaxy: a comprehensive approach for supporting accessible, reproducible, and transparent computational research in the life sciences. Genome Biol 2010; 11: R86. doi: 10.1186/gb-2010-11-8-r86 PMID: 20738864

46. Blankenberg D, Von KG, Coraor N, Ananda G, Lazarus R, Mangan M, et al. Galaxy: a web-based genome analysis tool for experimentalists. Curr Protoc Mol Biol 2010; 19.10: 1–21.

47. Giardine B, Riemer C, Hardison RC, Burhans R, Elnitski L, Shah P, et al. Galaxy: a platform for interactive large-scale genome analysis. Genome Res 2005; 15: 1451–1455. PMID: 16169926

48. Robinson MD, McCarthy DJ, Smyth GK. edgeR: a Bioconductor package for differential expression analysis of digital gene expression data. Bioinformatics 2010; 26: 139–140. doi: 10.1093/bioinformatics/btp616 PMID: 19910308

49. Hsu CY, Wu CW, Talaat AM. Genome-Wide Sequence Variation among *Mycobacterium avium* Subspecies *paratuberculosis* Isolates: A Better Understanding of Johne's Disease Transmission Dynamics. Front Microbiol 2011; 2: 236. doi: 10.3389/fmicb.2011.00236 PMID: 22163226

50. Benjamini Y, Hochberg Y. Controlling the False Discovery Rate: A Practical and Powerful Approach to Multiple Testing. Journal of the Royal Statistical Society Series B (Methodological) 1995; 57: 289–300.